

Cavity enhancement of resonant frequencies in semiconductor lasers subject to optical injection

T. B. Simpson

JAYCOR, P.O. Box 85154, San Diego, California 92186-5154

J. M. Liu

Department of Electrical Engineering, University of California, Los Angeles, Los Angeles, California 90095-159410

K. F. Huang and K. Tai

Department of Electro-Physics, National Chiao Tung University, Hsinchu, Taiwan

C. M. Clayton, A. Gavrielides, and V. Kovanis

Nonlinear Optics Center, Phillips Laboratory, Kirtland AFB, New Mexico 87117-5776

(Received 21 July 1995)

The injection of an optical signal into a semiconductor laser biased near or above the lasing threshold modifies the coupling between the free carriers and the intracavity field. The detuning between the frequency of the injected signal and the free-running oscillation frequency and the ratio of the photon lifetime to the carrier lifetime are key parameters in determining the enhancement of the carrier-field resonant coupling frequency and the stability of the output field. Experimental results using a vertical cavity surface emitting laser biased near threshold are in agreement with calculations using a lumped-element oscillator model.

PACS number(s): 42.55.Px, 42.65.Hw, 42.65.Ky, 42.70.Nq

Semiconductor lasers subject to external optical injection are being studied as a model nonlinear dynamical system and for their potential in optical communication and processing applications. External optical signals can induce stable and unstable injection locking [1], chaotic dynamics and multi-wave mixing [2,3], and mode hopping [4], depending on the amplitudes of the injected and oscillating fields and the frequency offset between them. These various characteristics have all been recovered in lumped-circuit oscillator models of the semiconductor laser subject to external injection. Recently, an amplifier model was used to describe some novel features in the optical spectra of a vertical cavity surface emitting laser (VCSEL) under strong optical injection [5]. The model predicted that stimulated emission and absorption due to the coherent transfer of energy significantly enhanced the semiconductor response and produced new resonances in the optical spectrum that are distinct from the relaxation resonances typically observed in semiconductor lasers. Here, we show that the laser cavity plays a major role in the generation of the new resonances and in the enhancement of the modulation bandwidth, and that the new resonances can be related back to the relaxation resonances observed in free-running semiconductor lasers.

In our analysis we will consider a single-mode semiconductor laser subject to external optical injection [3,6,7]. We will consider two external fields, a strong injection field that satisfies the conditions for injection locking, and a weak field that can be used as a linear probe. The interaction can be described by two coupled equations:

$$\begin{aligned} \frac{dA}{dt} = & -\frac{\gamma_c}{2}A + i(\omega_L - \omega_c)A \\ & + \frac{\Gamma}{2}(1 - ib)gA + \eta(A_i + A_i e^{-i\Omega t}), \end{aligned} \quad (1)$$

$$\frac{dN}{dt} = \frac{J}{ed} - \gamma_s N - \frac{2\epsilon_0 n^2}{\hbar \omega_L} g |A|^2, \quad (2)$$

where A is the total complex intracavity field amplitude at the locked oscillating frequency ω_L , γ_c is the cavity decay rate, ω_c is the longitudinal mode frequency of the cold laser cavity, Γ is the confinement factor, b is the linewidth enhancement factor, g is the gain coefficient, A_i and A_i are the amplitudes of the strong injection signal at the locking frequency and the weak probe signal at $\omega_L + \Omega$, respectively, η is the coupling rate, N is the carrier density, J is the injection current density, e is the electronic charge, d is the active layer thickness, γ_s is the spontaneous carrier decay rate, and n is the refractive index of the semiconductor medium. The gain is assumed to obey a linear dependence on deviations of both the carrier density and the circulating photon density about steady-state values [7].

Steady-state values for the circulating field are obtained by setting the derivative terms and A_i equal to zero. The locked phase of the oscillating field, ϕ_L , relative to the phase of the injection field, is obtained through the relation

$$\omega_L - \omega_0 = b\delta/2 - bU + V. \quad (3)$$

Here, ω_0 is the optical frequency of the free-running laser, $U = \eta|A_i/A_L|\cos\phi_L$ and $V = \eta|A_i/A_L|\sin\phi_L$, where A_L is the steady-state amplitude of the injection-locked circulating field. The gain defect $\delta = \gamma_c - \Gamma g_0$, where g_0 is the steady-state gain of the free-running laser, can be important when the free-running laser is biased below threshold. The free-running coherent field amplitude, A_0 , and A_L are related through

$$|A_0^2/A_L^2| = \frac{1 - X\gamma_s/\gamma_{nL}}{1 + X} \quad (4)$$

where the factor, X , is given by

$$X = \frac{(2U - \delta)\gamma_{nL}}{(\gamma_c - 2U)\gamma_{nL} + \gamma_s\gamma_{pL}}. \quad (5)$$

Here,

$$\gamma_{nL} = \frac{2n^2\epsilon_0}{\hbar\omega_L}|A_L|^2g_n \quad \text{and} \quad \gamma_{pL} = -\frac{2n^2\epsilon_0}{\hbar\omega_L}|A_L|^2\Gamma g_p, \quad (6)$$

where g_n and g_p are the differential gain and the nonlinear gain parameters defined as the derivatives of g with respect to the carrier density and the photon density, respectively, evaluated at the operating point [7]. When the free-running laser is biased below threshold, $|A_0^2/A_L^2| \approx 0$.

With these definitions, we can find the perturbations induced by the weak injected field. The weak field induces a regeneratively amplified (RA) sideband, A_r , at the injection frequency, $\omega_L + \Omega$, and a four-wave-mixing (FWM) sideband, A_f , at $\omega_L - \Omega$. In the perturbation limit:

$$\begin{aligned} \frac{A_r}{A_i} = \frac{\eta}{D} \{ & (\gamma_s + \gamma_{nL} - i\Omega)[U - i(\Omega - V)] \\ & + \frac{1}{2}(1 + ib)(\gamma_c\gamma_{nL} + \gamma_s\gamma_{pL} - 2U\gamma_{nL} - i\Omega\gamma_{pL}) \}, \end{aligned} \quad (7)$$

$$\frac{A_f}{A_i} = -\frac{\eta}{D^*} \{ \frac{1}{2}(1 - ib)(\gamma_c\gamma_{nL} + \gamma_s\gamma_{pL} - 2U\gamma_{nL} + i\Omega\gamma_{pL}) \}, \quad (8)$$

$$\begin{aligned} D = & (\gamma_s + \gamma_{nL} - i\Omega)[(U - i\Omega)(U + \gamma_{pL} - i\Omega) \\ & + V(V + b\gamma_{pL})] + (U + bV - i\Omega)(\gamma_c - 2U - \gamma_{pL})\gamma_{nL}. \end{aligned} \quad (9)$$

Measured optical sidebands are proportional to the squared magnitude of A_r and A_f . In addition, the spontaneous emission noise spectrum is proportional to the sum of the squared magnitudes of A_r and A_f [8]. This is because the spontaneous emission effectively acts as a weak external optical source. Therefore, this modeling also gives the sideband spectra due to amplified spontaneous emission and, for simplicity, we analyze the problem from this viewpoint. These equations simplify to the appropriate expressions for the free-running semiconductor laser when $U = V = 0$ and $A_L = A_0$, $\gamma_{nL} = \gamma_n$, and $\gamma_{pL} = \gamma_p$, the respective free-running values [7]. Under optical injection, D can be 0 and unstable and chaotic dynamics can ensue [2,3,9]. Here, we are primarily interested in the offset frequencies of the resonances and defer consideration of their stability.

When the free-running laser is biased below threshold and is subjected to a near-resonant locking field, the limit $|A_0^2/A_L^2| \ll 1$, and $\gamma_c \gg 2U$ and γ_s , then $U \approx \delta/2 + \gamma_c\gamma_{nL}/2\gamma_s$. In this limit, Eqs. (7) and (8) can be solved to show that the RA term dominates the FWM term. If the gain defect, δ , is large compared to γ_s and V , the central peak of the RA spectrum is shifted from the free-running spectrum. The difference between the two in the weak-locking, large- δ limit has maxima and minima shifted from the free-running frequency by $-\gamma_s[1/b \pm (1 + 1/b^2)^{1/2}]$, the same as predicted

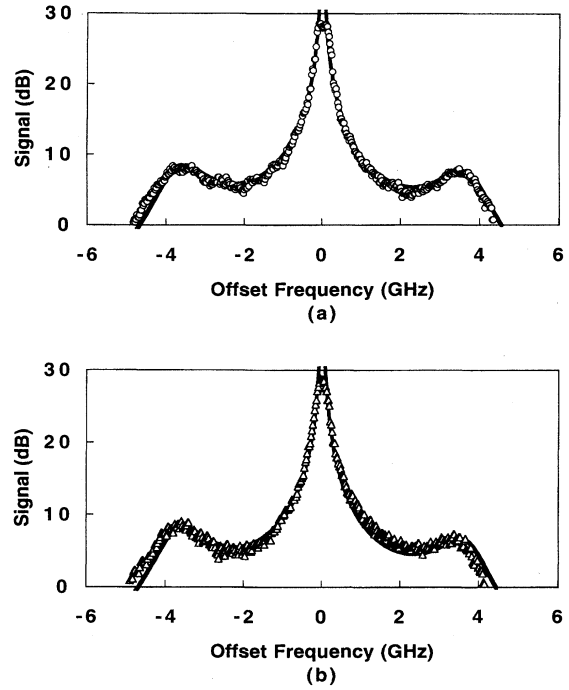


FIG. 1. (a) Optical spectrum of the free-running VCSEL biased well above threshold and (b) the regeneratively amplified spectrum due to the injection of a weak optical probe. The experimental data are compared with the calculated spectra using the parameters listed in the text.

by the amplifier analysis [5]. However, Eq. (7) predicts that the amplifier analysis is inadequate when the free-running laser is near or above threshold and/or when V becomes comparable to δ . As the injecting field is increased so that U and V dominate the other rates, except for γ_c , the RA term contains a strong resonance at $\Omega \approx -V = \omega_0 - \omega_L - b\gamma_c\gamma_{nL}/2\gamma_s$. The corresponding resonance at positive frequencies is much weaker due to a canceling term, $\Omega - V$, in the numerator. The magnitude of the shift is proportional to the circulating locked power, due to the coherent field-induced carrier decay rate, γ_{nL} . Unlike the amplifier analysis, there is a multiplicative factor of approximately $b\gamma_c/2\gamma_s$ for the resonance shift. This factor is typically on the order of 100–1000 in semiconductor lasers. When $\gamma_c \gg \gamma_s$, a large shift in the resonance can be observed even if $\gamma_s \gg \gamma_{nL}$.

To verify these predictions, we have investigated a VCSEL. Many of the characteristics of this VCSEL have been described previously [10,11]. All measurements reported here were made at low output power, under operating conditions where the VCSEL displayed single-mode operation and no significant transverse profile variations from effects such as thermal lensing or spatial hole burning. Figure 1 shows the output spectrum and the RA spectrum when the laser is biased at 4.8 mA, well above the threshold value of 4.2 mA. Total output power at this injection current is ≈ 0.35 mW and the coherent output power is ≈ 0.3 mW. Here, we can determine the key dynamic parameters of the laser from its spectra. Figure 1 shows the good agreement between data and model that is achieved using the determined parameters,

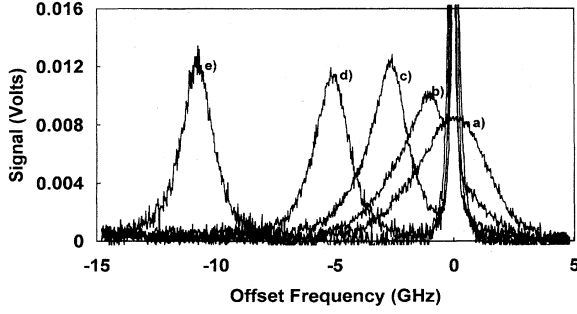


FIG. 2. Representative optical spectra of the free-running VCSEL biased just below threshold (a), and under increasing injected power from a narrow-band laser tuned to the free-running oscillation frequency (b)–(e). The injected power ratio of (b):(c):(d):(e) is 1:10:100:1000.

$b=6$, $\gamma_c=5.5 \times 10^{11} \text{ s}^{-1}$, $\gamma_s=5 \times 10^9 \text{ s}^{-1}$, $\gamma_n=3.5P \times 10^9 \text{ s}^{-1}$, and $\gamma_p=5.3P \times 10^9 \text{ s}^{-1}$. P in the formulas refers to the coherent output power in milliwatts, and the uncertainty for the parameters is $\pm 20\%$. The enhancement factor for the frequency shifts, relative to the amplifier case, is approximately 330.

For the injection-locking measurements, the bias current was set to 3.9 mA and the output from a tunable, narrow linewidth, low noise, external cavity laser (New Focus Model 6126) was injected into the VCSEL. Output power from the free-running VCSEL was $\approx 0.02 \text{ mW}$. Below threshold operation insured that $|A_0^2/A_L^2| \ll 1$. Here, we concentrate on optical injection at the free-running frequency. Consistent results were obtained for detuned injection. Figure 2 shows free-running and injection-locked optical spectra taken with a high finesse optical spectrum analyzer (Newport Model SR-240C) with $\approx 60 \text{ MHz}$ resolution. The resonance feature shifts to lower frequencies as the injection power increases.

Features from these spectra can be compared with the predictions of the model. The injection-locked output power

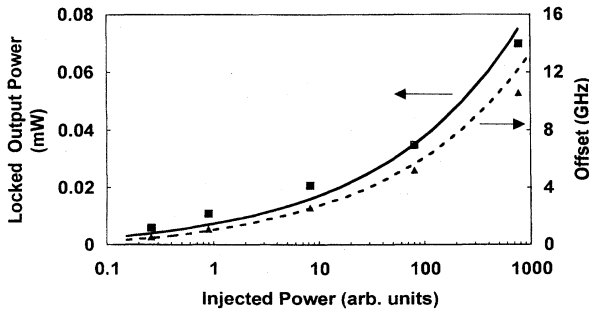


FIG. 3. The dependence of the injection-locked power, (\square) data and (—) model, and the shift of the resonance from the free-running frequency, (\triangle) data and (---) model, for the VCSEL biased just below threshold when subject to an injected signal at the free-running oscillation frequency.

can be determined from the spectra and the measured output power. Figure 3 shows the dependence of the injection-locked coherent power and the frequency shift of the resonance on the power injected into the VCSEL. Because we are unable to independently determine the coupling parameter, η , we can only make a relative measurement of the injection power, and the relative uncertainty is $\pm 50\%$. Using the experimentally determined parameters, model calculations for both the injection-locked coherent power and the frequency shift are in good agreement with the data. At high injection power levels, the offset frequency scales linearly with the injection-locked coherent power, and both scale with the cube root of the injected power. Even at the highest injected power measured, where the injection-locked coherent power is $\approx 0.07 \text{ mW}$, the field-induced enhancements of the decay rate are $\gamma_{nL} \approx 0.05 \gamma_s$ and $\gamma_{pL} \approx 0.075 \gamma_s$. These values coincide with the expected values at the lower operating power.

The modulation and noise spectra of the injection-locked laser are more complicated than the free-running spectra due, in part, to the dependence of the field amplitude on the locked phase. If the locking frequency is detuned from the free-running frequency so that $\phi_L \neq 0$, the amplitude becomes decoupled from the phase of the locking field, as is the case in the free-running laser. The correspondence between the new resonance peaks and the resonance peaks of an above threshold, free-running laser is more direct. The resonance peaks of the free-running laser are determined by the relaxation resonance frequency, $\Omega_r = (\gamma_c \gamma_n + \gamma_s \gamma_p)^{1/2}$, and the damping rate, $\gamma_r = \gamma_s + \gamma_n + \gamma_p$ [7]. For the $\phi_L = 0$ locked laser,

$$\Omega_{rL}^2 = \gamma_c \gamma_{nL} + \gamma_s \gamma_{pL} + (\gamma_s - \gamma_{nL})U, \quad (10)$$

$$\gamma_{rL} = \gamma_s + \gamma_{nL} + \gamma_{pL} + U. \quad (11)$$

Both Ω_{rL} and γ_{rL} show the direct modification due to the enhancement of the circulating coherent power under injection-locked operation. In addition, there are the terms proportional to U . These terms dominate the changes over a wide range of injection levels. More generally, when $\phi_L \neq 0$, there is a complicated dependence on both U and V which can lead to the destabilization of the laser as well as the enhancement of the modulation bandwidth. It is this complex coupling, involving both phase and amplitude modifications due to the strong injection-locking field, that dominates the shift in the resonance frequencies and their damping characteristics, not a simple enhancement of stimulated emission and absorption rates.

The lumped-element analysis of laser oscillation assumes that spatial effects can be averaged over the mode profiles. It has given excellent quantitative agreement with a wide variety of single-mode semiconductor lasers, including Fabry-Pérot edge emitting lasers with large output coupling [3,7]. The linearized treatment, like that given here, fails to accurately reproduce the central linewidth of the free-running laser and, more generally, the dynamics whenever a resonance

becomes unstable, but it shows good accuracy in the prediction of the positions and shifts of the resonance frequencies. The laser cavity strongly enhances the frequency shifts induced by the injection field beyond what is expected from the increased stimulated emission due to the stronger oscillating field. Phase and amplitude characteristics must be ana-

lyzed for a detailed quantitative understanding of the spectral features.

The authors would like to thank Dr. Tim Day for the loan of the New Focus tunable laser. The work of T.B.S. and J.M.L. was supported by the U.S. Air Force's Phillips Laboratory under Contract No. F29601-94-C-0166.

-
- [1] I. Petitbon, P. Gallion, G. Debarge, and C. Chabran, *IEEE J. Quantum Electron.* **24**, 148 (1988).
 - [2] J. Sacher, D. Baums, P. Panknin, W. Elsässer, and E.O. Göbel, *Phys. Rev. A* **45**, 1893 (1992).
 - [3] T.B. Simpson, J.M. Liu, A. Gavrielides, V. Kovanis, and P.M. Alsing, *Phys. Rev. A* **51**, 4181 (1995).
 - [4] P. Schanne, H.J. Heinrich, W. Elsässer, and E.O. Göbel, *Appl. Phys. Lett.* **61**, 2135 (1992).
 - [5] C.W. Lowry, F. Brown de Colstoun, A.E. Paul, G. Khitrova, H.M. Gibbs, J.W. Grantham, R. Jin, D. Boggavarapu, S.W. Koch, M. Sargent III, T.M. Brennan, and B.E. Hammons, *Phys. Rev. Lett.* **71**, 1534 (1993).
 - [6] T.B. Simpson and J.M. Liu, *J. Appl. Phys.* **73**, 2587 (1993).
 - [7] J.M. Liu and T.B. Simpson, *IEEE J. Quantum Electron.* **30**, 957 (1994).
 - [8] T.B. Simpson and J.M. Liu, *Opt. Commun.* **112**, 43 (1994).
 - [9] J.R. Tredicce, F.T. Arecchi, G.L. Lippi, and G.P. Puccioni, *J. Opt. Soc. Am. B* **2**, 173 (1985).
 - [10] H.M. Chen, K. Tai, K.F. Huang, Y.H. Kao, and J.D. Wynn, *J. Appl. Phys.* **73**, 16 (1993).
 - [11] K. Tai, Y. Lai, K.F. Huang, T.C. Huang, T.D. Lee, and C.C. Wu, *Appl. Phys. Lett.* **63**, 2624 (1994).